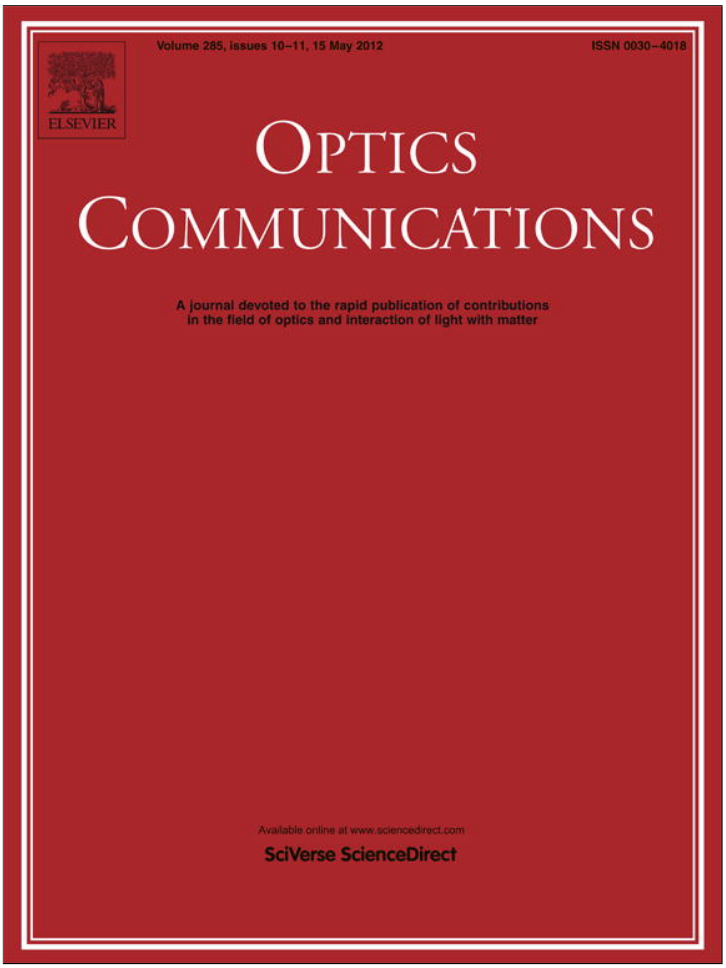

Optics Communications 285 (2012) 2627–2631

Contents lists available at SciVerse ScienceDirect

Optics Communications

journal homepage: www.elsevier.com/locate/optcom

Ar plasma waveguide produced by a low-intensity femtosecond laser

Guanglong Chen [a], Xiaotao Geng [b], Tawfik Walid Mohamed [b], Hongxia Xu [a], Yiming Mi [a], Jaehoon Kim [c], Dong Eon Kim [b,*]

[a] School of fundamental studies, Shanghai University of Engineering Science, Shanghai 201620, China
[b] Department of Physics, Center for Attosecond Science and Technology (CASTECH), and Max Planck Center for Attosecond Science (MPC-AS), Pohang University of Science and Technology (POTECH), Pohang 790-784, South Korea
[c] Medical IT Fusion Research Division, Korea Electrotechnology Research Institute, Ansan 426-170, South Korea

ARTICLE INFO

Article history:
Received 14 July 2011
Received in revised form 29 December 2011
Accepted 4 February 2012
Available online 18 February 2012

Keywords:
Plasma waveguide
Ar cluster
Femtosecond laser

ABSTRACT

Using the interaction of a low-intensity femtosecond laser pulse (30 fs, 6×10^{15} Wcm^{-2}) with argon cluster jet produced from a slit nozzle, we experimentally probe the formation of a uniform plasma waveguide by the interferogram analysis. The results about evolution of plasma channel demonstrate that it is feasible to produce the plasma waveguide for an fs laser pulse of low-intensity. It takes tens of nanoseconds to form a plasma waveguide. The simulation by one-dimensional Gaussian plasma hydrodynamic expansion model indicates that the temperature of plasma channel is not high under this condition. Thus it takes tens of nanoseconds to form a plasma waveguide.

1. Introduction

Since a clustered gas target possesses the advantage of both solid target and gas target and exhibits the high absorption of laser pulse energy, it has served as good sample in the laser–matter interaction in the past decade. Up to now, there have already existed many important findings, such as the deuterium–deuterium nuclear fusion and the production of high energy ions [1,2]. From the successful laser–cluster interaction model proposed by Ditmire et al., the high energy ions and high charge states of ions result from the resonant absorption of the large-size clusters (which are produced under high backing pressure) [3]. Thus a clustered gas produces more electrons than a non-clustered gas under a given laser condition and indicates the better choice for channel generation [4,5]. The investigation of plasma channels has been an active area of research for high harmonic generation (HHG) [6], laser acceleration [7,8], and x-rays laser [9]. However, in the past, for a traditional laser-induced plasma channel, a gas has been usually used as an interaction target [10,11]. As discussed in Ref [5], there are some significant drawbacks for gas target. For example, because the initial electron density is not enough to make efficient collisional breakdown for channel generation, the typical central electron density of waveguide formed from plasma channel is higher than ~5×10^{18} cm^{-3}, which is not optimum for some applications such as HHG, laser acceleration, etc. (while in our work as shown in Results and discussion, the central density is estimated to be 1.4×10^{18} cm^{-3} when a clustered gas target is used). Also the requirement for adequate ionization and heating for channel formation demands the use of high energy, long duration pulses from an auxiliary laser [5]. Using the high energy absorption of clustered gas, Ditmire et al. demonstrated the formation of a plasma waveguide by the interaction of a ps laser pulse with an argon cluster jet at a backing pressure of 55 bars [4]. In their work, two ps laser pulses (i.e., a prepulse and a main pulse) were used. Firstly, the prepulse with an intensity of ~10^{13} Wcm^{-2} passed through the cluster jet and was used to disassemble the clusters to be atoms on its way. Then a main pulse with an intensity of 5×10^{15} Wcm^{-2} (25 mJ, 2 ps) was sent to the same part of the cluster jet and interacted with the remaining annulus of clusters and the center where no cluster exists. Due to the resonant absorption by clusters, the remaining annulus produced more electrons than the center. A plasma waveguide with low-density at the center and maximum density around peripheral was then formed 40 ps later. However, no plasma waveguide was demonstrated when only the main laser pulse was used in their work. In order to know whether a plasma waveguide can be produced only using the main laser pulse of low intensity, in this work we attempted to use only one laser pulse of similar intensity (15 mJ, 6×10^{15} Wcm^{-2}), but of 30 fs pulse duration to interact with an argon cluster jet and explore the formation of a plasma waveguide. It is noted that the motivation for using an fs laser pulse with low intensity to form plasma waveguide comes from our experimental goal for generation of the HHG from ions by fs laser pulse, in which the fs laser pulse is split into two pulses. One is for the generation of plasma waveguide, the other is for the HHG from the interaction of fs laser with ions. The argon cluster jet was produced from a slit nozzle at the backing pressure of 50 bars. The time-resolved interference measurements were conducted and the interferogram analysis

* Corresponding author.
E-mail address: kimd@postech.ac.kr (G. Chen).

0030-4018/$ – see front matter © 2012 Elsevier B.V. All rights reserved.
doi:10.1016/j.optcom.2012.02.005

indicated that a uniform plasma waveguide was clearly formed. Obviously, the plasma waveguide in our case resulted from plasma hydrodynamic expansion, which was different from that reported in Ref. [4], as discussed above. Thus the plasma waveguide formation in our work needs a long time (~20 ns). The simulation using a one-dimensional Gaussian plasma expansion model was made, indicating that the temperature of plasma channel could not be high.

2. Experimental setup

The schematic diagram of the experimental setup is shown in Fig. 1. A pulsed valve (Parker series 99) with a 0.5 mm diameter orifice was used (1/15 Hz repetition rate is set). A slit nozzle (0.5×5 mm^2) with the length of 5 mm was directly connected to the pulsed valve. A pressure of 3×10^{-5} Torr in a chamber ($59\times53\times30$ cm^3) was maintained before the operation of the pulsed valve. An Argon cluster jet was produced from the adiabatic expansion of a high pressure argon gas into vacuum through the slit nozzle. Thus the cross-section shape of cluster jet was square and its width at 2 mm above the slit nozzle along the main laser pulse was about 2 mm. In this work, the backing pressure was kept to be 50 bars and Rayleigh scattering measurement was used to observe the cluster formation. The average cluster size was estimated to be about 5 nm based on our previous experimental result [12].

The femtosecond laser utilized in our experiment was a Ti:sapphire laser system based on chirped pulse amplification, producing 800 nm pulses at a 10 Hz repetition rate. The energy of a pump pulse delivered to the gas plume was estimated to be about 15 mJ and the pulse duration was about 30 fs. As shown in Fig. 1, the main laser beam was focused using a lens with a focal length of 70 cm and the focal spot at 2 mm downstream from the slit nozzle was about 100 μm in diameter, yielding a peak laser intensity of about 6×10^{15} Wcm^{-2}. Meanwhile a small portion of the laser beam leaked from a 95% reflective mirror was sent across the cluster jet along the slit nozzle direction but transverse to the main laser beam, as shown in Fig. 1. The probe beam was then analyzed in a Michelson interferometer which has a roof prism in one leg so that a part of the probe beam that traversed the plasma channel was interfered with other part of probe beam that passed below the plasma. The interferogram encodes information on the phase shift for a cylindrically symmetric plasma. The electron density of the plasma can be extracted from the resulting interferogram by Abel inversion. By varying the delay of the probe beam with respect to the main laser beam using the delay arm, the evolution of the laser plasma expansion was investigated.

3. Results and discussion

To investigate the evolution of the plasma channel produced by the interaction of fs intense laser with an argon cluster jet, we conducted a series of the time-resolved interference experiments to probe the evolution of plasma density. Firstly we obtained the femtosecond interferogram at a delay time of 4 ns between the probe beam and the main beam. Typical interferograms are shown in Fig. 2. The direction of the main laser propagation and the center of the cluster jet are indicated by two inserted red arrows, respectively. From Fig. 2(a), the interference fringes are smeared in the region of a laser–cluster jet interaction and the plasma is observed clearly from the shift of interference fringes. The plasma length is about 1.2 mm and a little shorter than the width of cluster jet (2 mm), which results from the high absorption of laser energy by the cluster jet as discussed. The electron density at the center of cluster jet is extracted using an interferogram analysis code. The results are shown also in Fig. 2. There exists the maximum electron density nearby the axis of plasma and the electron density profile rapidly decreases as the radius of plasma increases. The maximum density is about 1.8×10^{19} cm^{-3} at the radial position of 6 μm, while the density is almost zero at the radial position of 50 μm. The width of the plasma at half maximum of a density is about 40 μm.

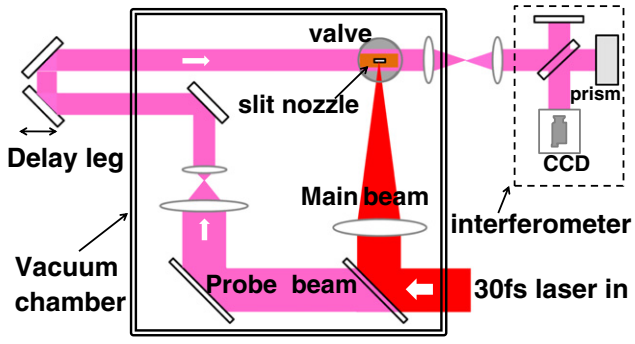

Fig. 1. Schematic diagram of the experimental setup.

Then we have also performed the investigation of femtosecond interferograms at the delay time of 12 ns. A typical interferogram is shown in Fig. 2(c). Compared with that in Fig. 2(a), the plasma width becomes larger and the plasma waveguide can be observed even though it is not clearly visible. To get more information of the waveguide, the profile of electron density at the axis of plasma was extracted and shown in Fig. 2(d). From Fig. 2(d), it is found that the maximum electron density (8.0×10^{18} cm^{-3}) is about 26 μm off axis and its electron density is a little higher than the electron density on axis (6.7×10^{18} cm^{-3}). That is to say, the plasma has the lower density on axis and higher density at the edge. We note that the formation of a hollow density profile starts. Meanwhile it is noted that the maximum density (8.0×10^{18} cm^{-3}) is lower than 1.8×10^{19} cm^{-3} at the delay time of 4 ns. This results from the plasma expansion. We estimate the velocity of plasma expansion using the positions (18 and 37 μm for 4 and 12 ns, respectively) of the half of the maximum density. The expansion velocity is about 2.4×10^{5} cms^{-1}.

The formation of a plasma waveguide was demonstrated by the femtosecond interferogram at delay time of 20 ns, as shown in Fig. 2(e). Fig. 2(e) indicates that the diameter of plasma becomes larger compared to that in Fig. 2(d) due to further plasma expansion. Similarly, to show the formation of the waveguide more clearly, the electron density profile was extracted from the interferogram using the Abel inversion technique and shown in Fig. 2(f). From Fig. 2(f), the profile of a maximum density at edge and a lower density on axis is clearly observed. The profile is obviously different from that in Fig. 2(b) and (d). The electron density on axis of plasma is estimated to be 1.4×10^{18} cm^{-3} and the electron density at edge of plasma is about 5.5×10^{18} cm^{-3}. The difference in density between on axis and at edge is about 4.1×10^{18} cm^{-3}. This means that a good waveguide is formed at a delay time of 20 ns. The radial position of the maximum density is 32 μm. Similarly the expansion velocity of plasma is estimated to be about 1.9×10^{5} cms^{-1} using the positions of half of the maximum density (37 and 52 μm) at 12 ns and 20 ns delay time. Obviously the velocity of plasma expansion is decreased, due to the plasma cooling during expansion. The electron density distribution of this channel along the direction of main laser beam is shown in Fig. 3. Fig. 3 shows clearly the formation of a hollow plasma channel (waveguide) with a nearly uniform radius. It is interesting to note that there exist some electrons at the entrance and the exit of the channel. This could be understood as follows. As known, the energy of ions and electrons produced from laser–cluster interaction is related to the cluster size and the laser intensity [3]. The distribution at the entrance could result from the low atom density and small cluster size at the edge of cluster jet and thus the corresponding plasma consists of ions (electrons) with low energy and has low expansion velocity. As for the distribution at the exit, it could result from the low laser intensity due to the absorption by cluster jet.

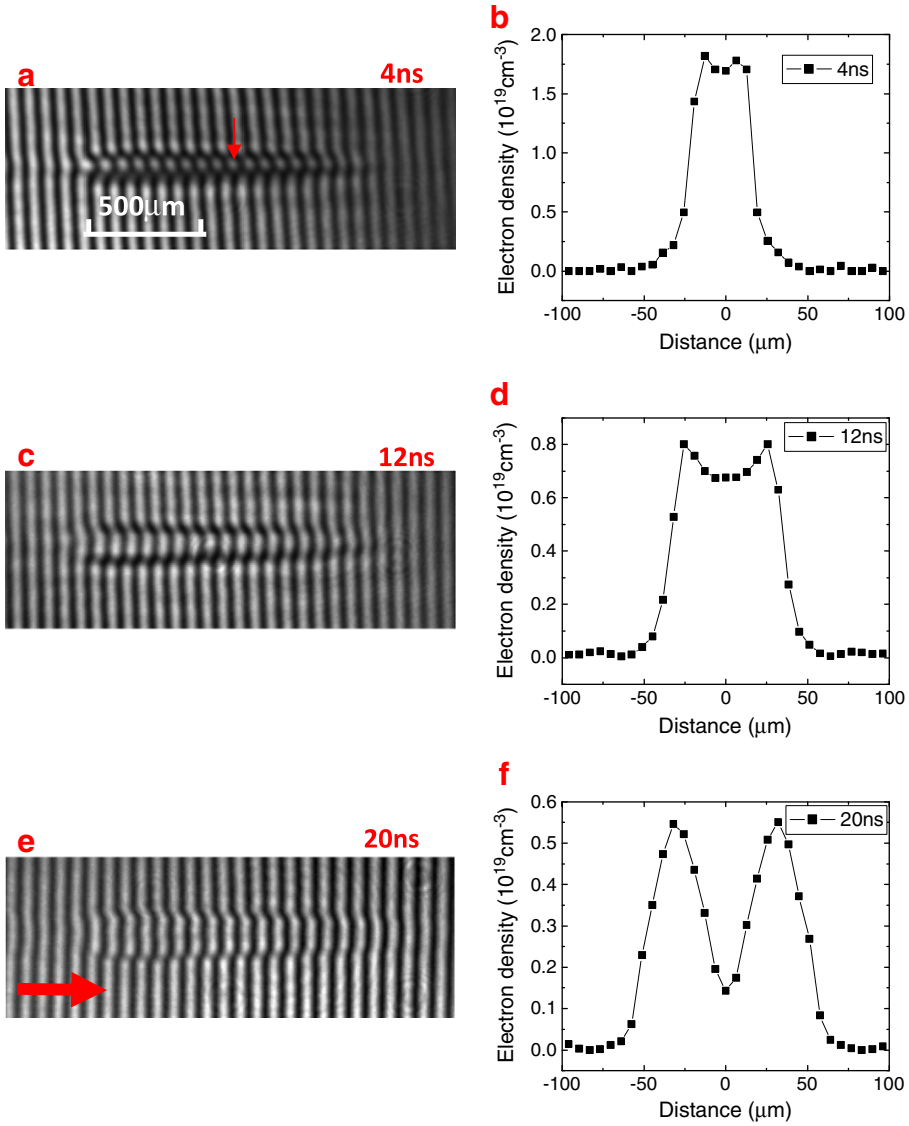

Fig. 2. Typical femtosecond interferograms and their corresponding profiles of electron density at the center of cluster jet at a delay time of 4 ns (a, b), 12 ns (c, d) and 20 ns (e, f). The direction of the main laser propagation and the center of the cluster jet are indicated by two inserted red arrows, respectively.

To further clearly show the evolution of the plasma channel, the cross sectional density profiles at delay times of 4, 12 and 20 ns are put together in Fig. 4. As shown in Fig. 4, as the plasma expands, the electron density at axis gradually decreases and the electron density at edge gradually becomes larger than that on axis. At a delay time of about 20 ns a plasma waveguide with an excellent hollow profile is formed.

To better understand the formation of waveguide, it is necessary to investigate the plasma temperature. We conducted a simulation for plasma expansion using a simple one-dimensional Gaussian plasma hydrodynamic expansion model in which the basic atomic processes relevant to ultra-cold plasmas were neglected [4,13]. The hydrodynamic expansion of plasma was investigated by its time-

Fig. 3. Electron density distribution of plasma at a delay time of 20 ns.

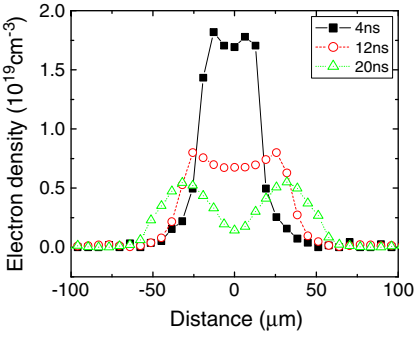

Fig. 4. Evolution of the cross section of electron density. The direction of the main laser propagation is perpendicular to the page.

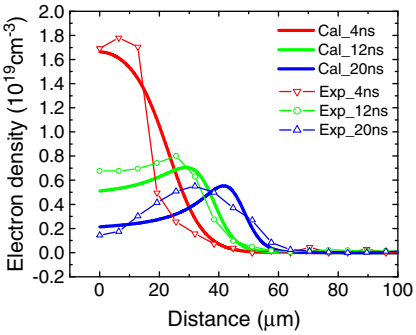

Fig. 5. Comparison of the experimental cross sectional density profiles of electron density with simulation results (solid lines) at delay times of 4, 12 and 20 ns for n_0 of 2.5×10^{19} cm^{-3}, $3kT_0/2$ of 1 eV, and R_0 of 20 μm. The direction of the main laser propagation is perpendicular to the page.

and space-resolved density evolution. A cylindrical geometry of plasma was assumed and the ideal gas equation of state ($P=n_ekT_e$, where P is the electron thermal pressures, T_e is the electron temperature and n_e is the electron density, respectively.) was used for the electrons. The mass conservation equation of the ions was given by $\frac{\partial n_i}{\partial t}=-\frac{1}{r}n_iv-n_i\frac{\partial v}{\partial r}-v\frac{\partial n_i}{\partial r}$ (where n_i is ion density and v is expansion velocity), the equation of the motion of the ions read $\frac{\partial v}{\partial t}=-v\frac{\partial v}{\partial r}-\frac{ZkT_e}{m_in_e}\frac{\partial n_e}{\partial r}-\frac{Zk}{m_i}\frac{\partial T_e}{\partial r}$ (where Z is the charge state of argon ion, m_i is the ion mass and k is the Boltzmann constant), and the energy equation was written to be $\frac{\partial T_e}{\partial t}=-\frac{4T_e}{3r}v$. Assuming that the initial fluid velocity v was equal to zero, the ion density and electron density were given by $n(x,\ t=0)=n_0\exp(-x^2/R_0^2)$ and the temperature of electrons was written as $T_e(x,t=0)=T_0\exp(-x^2/R_0^2)$ in the laser created Gaussian plasma. The charge state of argon was assumed to be +2 due to laser field ionization for our laser intensity based on the similar experimental conditions in Ref. [4]. We solved these equations and presented the calculated results in Fig. 5. As shown in Fig. 5, it is interesting to find that when the electron density n_0 of 2.5×10^{19} cm^{-3}, the electron temperature $3kT_0/2$ of 1 eV, and the radius of the plasma R_0 of 20 μm are used, the electron density profiles are in agreement with the experimental results. It is noted that the radius of the plasma is much smaller than the radius of laser focal spot (50 μm), which could result from the low laser intensity. From this result, the plasma temperature (1 eV) obviously seems to be low. We can understand this as follows: (1) the one-dimensional Gaussian plasma expansion model, i.e., pure hydrodynamics model neglects electron heat conduction and the radiation energy losses, which could induce the plasma cooling. That is to say, the decrease of plasma temperature actually results from the plasma expansion, heat conduction and the radiation energy losses, while in our calculation the decrease of plasma temperature results from only the plasma expansion. Thus the temperature drop should be underestimated in the calculation. The real temperature T_0 could be higher than 1 eV. (2) Based on the successful laser–cluster interaction model proposed by Ditmire et al., the high temperature of plasma due to the interaction of intense pulses with clusters results from the resonant absorption of clusters. It is also related to the laser pulse intensity and pulse duration. If the pulse duration is proper, the resonant absorption begins to occur near the peak of the pulse, which greatly enhances the cluster heating. Otherwise (the pulse duration is too long or too short), it is not helpful to produce a high temperature plasma. As reported in Ref. [14], Xe clusters produced by an expanding high-pressure (1 MPa) Xe gas into vacuum using a pulsed valve with an orifice diameter of 500 μm, 500 fs pulse duration at an intensity of 2×10^{17} Wcm^{-2} was the best for the production of high energy ions and high charge state. While for 20 fs pulse duration, even at a higher intensity of 5×10^{18} Wcm^{-2}, the mean ion energy was much lower than that for 500 fs pulse duration. Normally, the high intensity and the proper pulse duration are necessary for the production of higher charge states, i.e., plasma of higher temperature. In our case, the pulse duration is about 30 fs, which may not be sufficiently long for good resonant absorption of large clusters. Meanwhile our laser intensity is also low and not sufficient to help the energy coupling between laser fields and clusters. Considering these points the low temperature of plasma channel could be understood. It is the low temperature of plasma channel that leads to the slow evolution of plasma waveguide.

We note that for the plasma waveguide shown in Fig. 3, it is not difficult to find the tapering of the waveguide along the direction of channel, i.e., the propagation direction of the main laser pulse. In our experiment, the laser beam was focused by a lens with a focus length of 70 cm and the Rayleigh length was estimated to be about 10 mm. As mentioned above, the cluster jet was produced from a slit nozzle and the width of the laser–cluster interaction region was about 2 mm and was much shorter than the Rayleigh length. Thus this tapering should result from the decrease in the laser energy due to the absorption of cluster jet. If higher intensity is used, a more uniform and longer channel could be expected. This is because a high intensity will induce a self-focused propagation and thus could create a plasma waveguide with a longer length. As demonstrated in Ref. [5], by the self-focused propagation and strong absorption of on an intense fs laser pulse (25 mJ, 70 fs, 4×10^{17} Wcm^{-2}) in a clustered Ar gas jet, a long plasma channel of 10 mm was formed. They guided a laser pulse (40 mJ, 70 fs, 6×10^{17} Wcm^{-2}) using this channel. On the other hand, it is necessary to note that the high laser intensity will create the plasma channel of a higher temperature, and thus it will take a short time to form the plasma waveguide. For example, this time is about 3 ns in Ref. [5], which is much shorter than our results.

4. Conclusions

In conclusion, we experimentally created a uniform plasma channel using a femtosecond laser pulse of low intensity (6×10^{15} Wcm^{-2}) in interaction with argon cluster jet, and the interferograms of plasma channel were obtained at different delay times by femtosecond interference measurements. The interferogram analysis results clearly indicate the formation and evolution of a plasma waveguide. This work suggests a feasible scheme for the HHG experiments using plasma waveguide, in which an fs laser pulse can be split into two pulses, one for the generation of plasma waveguide, the other for the HHG from the interaction of fs laser with ions. Thus the complicated additional instrumentation for plasma waveguide could be avoided. However, it is necessary to note that the formation of plasma waveguide requires longer time (tens of nanosecond) due to the low plasma temperature for a low-intensity laser driven plasma.

Acknowledgements

This work has been supported in part by Global Research Laboratory Program [Grant No 2011-00131], by Leading Foreign Research Institute Recruitment Program [Grant No 2010-00471], by Max Planck POSTECH/KOREA Research Initiative Program [Grant No 2011-0031558] through the National Research Foundation of Korea(NRF) funded by the Ministry of Education, Science and Technology(MEST), by Natural Science Foundation of Shanghai, China (Grant No. 11ZR1414500) and by Discipline Development Program of Shanghai University of Engineering Science, China (Grant Nos. 11XK11 and 2011X34).

References

[1] T. Ditmire, J. Zweiback, V.P. Yanovsky, T.E. Cowan, G. Hays, K.B. Wharton, Nature (London) 398 (1999) 489.
[2] A. McPherson, B.D. Thmpson, A.B. Borisov, K. Boyer, C.K. Rhodes, Nature (London) 370 (1994) 631.
[3] T. Ditmire, T. Donnelly, A.M. Rubenchik, R.W. Falcone, M.D. Perry, Physical Review A 53 (1996) 3379.
[4] T. Ditmire, R.A. Smith, M.H.R. Hutchinson, Optics Letters 23 (1998) 322.
[5] V. Kumarappan, K.Y. Kim, H.M. Milchberg, Physical Review Letters 94 (2005) 205004.
[6] A. Emily, et al., Physical Review Letters 92 (2004) 033001.
[7] Y. Fukuda, et al., Physical Review Letters 103 (2009) 165002.
[8] P.M. Nilson, et al., New Journal of Physics 12 (2010) 045014.
[9] Y. Nagata, K. Midorikawa, S. Kubodera, M. Obara, H. Tashiro, K. Toyoda, Physical Review Letters 71 (1993) 3774.
[10] C.G. Durfee III, H.M. Milchberg, Physical Review Letters 71 (1993) 2409.
[11] A. Butler, D.J. Spence, S.M. Hooker, Physical Review Letters 89 (2002) 185003.
[12] Guanglong Chen, et al., Journal of Applied Physics 106 (2009) 5053507.
[13] G.L. Chen, et al., European Physical Journal D 47 (2008) 303.
[14] V. Kumarappan, M. Krishnamurthy, D. Mathur, Physical Review A 66 (2002) 033203.